

# Groundwater age, mixing and flow rates in the vicinity of large open pit mines, Pilbara region, northwestern Australia

Peter Cook<sup>1</sup> · Shawan Dogramaci<sup>2</sup> · James McCallum<sup>1</sup> · Joanne Hedley<sup>2</sup>

Received: 29 March 2016 / Accepted: 22 August 2016 / Published online: 8 September 2016  
© Springer-Verlag Berlin Heidelberg 2016

**Abstract** Determining groundwater ages from environmental tracer concentrations measured on samples obtained from open bores or long-screened intervals is fraught with difficulty because the sampled water represents a variety of ages. A multi-tracer technique (Cl,  $^{14}\text{C}$ ,  $^3\text{H}$ , CFC-11, CFC-12, CFC-113 and  $\text{SF}_6$ ) was used to decipher the groundwater ages sampled from long-screened production bores in a regional aquifer around an open pit mine in the Pilbara region of northwest Australia. The changes in tracer concentrations due to continuous dewatering over 7 years (2008–2014) were examined, and the tracer methods were compared. Tracer concentrations suggest that groundwater samples are a mixture of young and old water; the former is inferred to represent localised recharge from an adjacent creek, and the latter to be diffuse recharge. An increase in  $^{14}\text{C}$  activity with time in wells closest to the creek suggests that dewatering of the open pit to achieve dry mining conditions has resulted in change in flow direction, so that localised recharge from the creek now forms a larger proportion of the pumped groundwater. The recharge rate prior to development, calculated from a steady-state Cl mass balance, is 6 mm/y, and is consistent with calculations based on the  $^{14}\text{C}$  activity. Changes in CFC-12 concentrations with time may be related to the change in water-table position relative to the depth of the well screen.

**Keywords** Groundwater age · Mining · Groundwater recharge/water budget · Australia

## Introduction

Groundwater age (or residence time) can be estimated from measurements of environmental tracers in groundwater, involving comparison with known or reconstructed histories of tracer concentrations in rainfall. Carbon-14 has been used for this purpose for more than 40 years (Pearson and White 1967), enabling estimates of groundwater age over timescales between approximately 200 and 30,000 years. A much larger number of tracers is available for young (<60 year old) groundwater, with chlorofluorocarbons (CFCs), sulphur hexafluoride ( $\text{SF}_6$ ) and  $^3\text{H}$  the most widely used (e.g., Dunkle et al. 1993; Busenberg and Plummer 2000; Robertson and Cherry 1989; Fig. 1). Groundwater age determination allows estimation of horizontal and vertical groundwater flow velocities, and hence rates of groundwater recharge in both confined and unconfined aquifers (Dunkle et al. 1993; McMahon et al. 2011; Pearson and White 1967).

When using groundwater ages to estimate flow velocities, it is important to know the location within the flow systems from which the groundwater samples were drawn. Environmental tracer measurements are therefore easiest to interpret when they are obtained on groundwater collected from piezometers with short-screened intervals in steady-state flow fields (e.g., Cook et al. 1995). When samples are collected from short-screened piezometers, the vertical location of the sample is clear, and mixing between waters of different ages is minimised. However, production bores for irrigation, town water supply and mine-dewatering operations usually have long screened intervals, because they are constructed to maximise the volume of water that can be

✉ Peter Cook  
peter.cook@flinders.edu.au

<sup>1</sup> National Centre for Groundwater Research and Training (NCGRT), School of the Environment, Flinders University, GPO Box 2100, Adelaide, SA 5001, Australia

<sup>2</sup> Rio Tinto Iron Ore, 162–168 St Georges Tce, Perth, WA, Australia

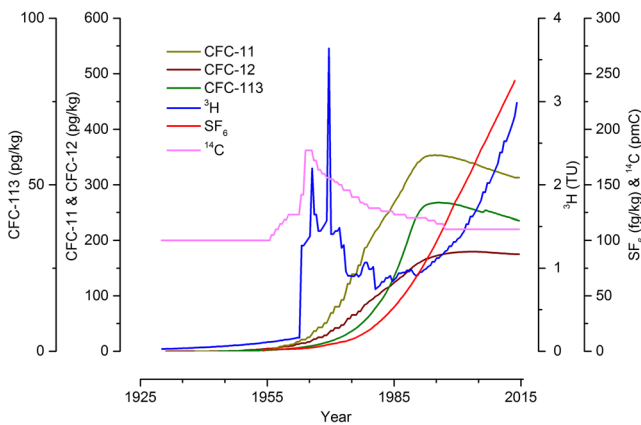


**Fig. 1** Atmospheric concentrations of environmental tracers in the Southern Hemisphere. CFC and  $\text{SF}_6$  curves are based on measured atmospheric concentrations at Cape Grimm, and a solubility at 24 °C and recharge elevation of 600 m AHD.  $^3\text{H}$  data are the average of measurements at Darwin and Perth (Tadros et al. 2014), decay-corrected to 2014.  $^{14}\text{C}$  data are based on Levin et al. (1992)

extracted. Pumping from long-screened wells can induce mixing between young water sourced from shallow depths and deeper, older water (Eberts et al. 2012; Visser et al. 2013; Jurgens et al. 2014). Mixing can also occur within the aquifer itself, and a number of recent studies have highlighted difficulties of interpreting environmental tracer data where mixing of water of different ages occurs (Varni and Carrera 1998; Weissmann et al. 2002; McCallum et al. 2014). Within steady flow fields, mixing occurs due to diffusion and dispersion, although it is likely that this is enhanced where changes in flow systems have occurred over time.

The ages within an aquifer are also dependent on the inflows and outflows of the system. In areas where inflows and outflows change with time, groundwater ages are transient (Cornaton 2012), which is often ignored when interpreting groundwater age data, but can be observed through the collection of environmental tracers over time intervals of decades (Manning et al. 2012; Massoudieh 2013). In environments where large changes in the system are occurring over short times, variations in age mixtures may be observable over shorter time frames, which is true in the case of heavily pumped systems (Leray et al. 2014). The observable changes will be dependent on the level of stress applied to the system, and how much the flow field is changed.

In this report, environmental tracer concentrations in a heterogeneous aquifer are examined, where long-screened wells installed for mine-dewatering produce samples that are mixtures of young and old water. Changes in tracer concentrations over time are also apparent, presumably induced by changes in flow fields caused by mine-dewatering operations. The aim of the study is to develop the conceptual model for flow at the site and how this may have changed over time, and to determine groundwater recharge mechanisms and constrain recharge rates.

## Background

### Chloride mass balance

Estimates of diffuse recharge are often obtained from a mass balance of chloride in groundwater and chloride in rainfall. Assuming that (1) rainfall (and dryfall) is the only source of chloride, (2) chloride behaves conservatively within the groundwater, (3) surface runoff is negligible, and (4) the catchment is in steady state, then the recharge rate ( $R$ ) can be estimated using:

$$R = \frac{c_P P}{c_R} \quad (1)$$

where  $c_P$  is the mean chloride concentration in rainfall,  $c_R$  is the chloride concentration in groundwater recharge, and  $P$  is the mean precipitation rate. If runoff occurs, then the chloride fallout ( $c_P P$ ) is reduced in proportion to the fraction of precipitation that leaves the catchment in runoff. Equation (1) has been widely applied to estimate rates of groundwater recharge, particularly in arid regions where other approaches are subject to large errors (Allison et al. 1994). The main limitations of the method are accurate estimation of chloride fallout, and the assumption of steady state. If steady-state conditions do not occur, and the catchment has undergone hydrological change, then Eq. (1) can still be used to estimate recharge rates prior to the hydrological change, provided that the groundwater sample was recharged prior to that event.

### Groundwater age and recharge

Groundwater age estimates can be obtained using a number of different tracers including  $^{14}\text{C}$ , CFCs,  $\text{SF}_6$  and  $^3\text{H}$ . Where samples are obtained from discrete points within an aquifer (such as wells with very short screens), then water ages can be directly used to estimate the groundwater recharge rate. If sampling occurs close to the water table then the recharge rate can be approximated by

$$R = \frac{z\varepsilon}{t} \quad (2)$$

where  $z$  is the depth of sampling,  $\varepsilon$  is the porosity, and  $t$  is the groundwater age (Solomon and Sudicky 1991). In an unconfined, wedge-shaped aquifer (where aquifer thickness increases linearly with distance downgradient), Eq. (2) will be correct irrespective of the depth of sampling. More generally, however, the relationship between recharge rate and groundwater age will depend on the aquifer geometry, and models have been developed that relate groundwater age and recharge for simple aquifer types (Vogel 1967; Cook and Bohlke 2000).

## Carbon-14

Carbon-14, with a half-life of 5,730 years, enables estimation of groundwater ages over time periods of approximately 200–30,000 years. It is formed naturally in the upper atmosphere by cosmic ray bombardment of  $^{14}\text{N}$ . In the atmosphere, most atmospheric  $^{14}\text{C}$  is in the form of  $^{14}\text{CO}_2$ . It is incorporated into groundwater during recharge, where most dissolved inorganic carbon occurs as  $\text{HCO}_3^-$ . Where  $\text{HCO}_3^-$  behaves conservatively (i.e., does not react with the aquifer matrix or undergo other chemical changes that affect the  $^{14}\text{C}$  activity), groundwater ages can be estimated from measured  $^{14}\text{C}$  concentrations using:

$$\frac{c}{c_0} = e^{-t\lambda} \quad (3)$$

where  $t$  is the apparent groundwater age,  $c$  is the measured  $^{14}\text{C}$  activity,  $c_0$  is the initial activity, and  $\lambda = 1.21 \times 10^{-4} \text{ y}^{-1}$  is the radioactive decay constant. The initial activity is often considered to be the activity of atmospheric  $\text{CO}_2$ , which is often assumed to be 100 pmC. However, it is common for rock–water interactions to alter the  $^{14}\text{C}$  activity of the groundwater. Measurement of the stable isotope  $^{13}\text{C}$  and other aquifer chemistry sometimes allows correction to be made for variations in  $^{14}\text{C}$  activities resulting from chemical processes (Ingerson and Pearson 1964; Tamers 1967).

A commonly used correction scheme is based on the measured  $^{13}\text{C}$  ratio and assumed  $^{13}\text{C}$  values and  $^{14}\text{C}$  activities of soil  $\text{CO}_2$  and carbonate minerals:

$$A_{\text{corr}} = A_{\text{T}} \left[ \frac{A_{\text{m}}}{A_{\text{g}}} + \left( 1 - \frac{A_{\text{m}}}{A_{\text{g}}} \right) \left( \frac{(\delta_{\text{T}} - \delta_{\text{m}})}{(\delta_{\text{g}} - \delta_{\text{m}})} \right) \right] \quad (4)$$

where  $A$  refers to the  $^{14}\text{C}$  activity,  $\delta$  refers to the  $\delta^{13}\text{C}$  value, subscripts T, m and g refer to total TDIC, carbonate minerals and soil gas, respectively, and  $A_{\text{corr}}$  is the corrected  $^{14}\text{C}$  activity. This correction is generally known as the Pearson model (Ingerson and Pearson 1964; Clark and Fritz 1997).  $A_{\text{corr}}$  is then used in place of the measured  $^{14}\text{C}$  activity in Eq. (3).

## CFCs and $\text{SF}_6$

Chlorofluorocarbons and  $\text{SF}_6$  are synthetic organic compounds that are produced for a range of industrial and domestic purposes. They have relatively long residence times in the atmosphere, and so their atmospheric concentrations are uniform over large areas. Atmospheric concentrations of CFC-11, CFC-12 and CFC-113 increased in the atmosphere after the 1950s, to peak in concentration between 1994 and 2002 (different CFCs peaked at different times). Since that time, concentrations have decreased between 3 and 13 %. In contrast, atmospheric concentrations of  $\text{SF}_6$  are still increasing (Fig. 1). Comparison of concentrations of CFC and  $\text{SF}_6$  in

groundwater with atmospheric concentrations indicates the time at which a groundwater sample was last in contact with the atmosphere, and hence the groundwater age, assuming that all water in the sample is of a single age.

There are a number of difficulties in using CFCs and  $\text{SF}_6$  for groundwater dating. As these compounds are gases with relatively low solubility in water, contact with the atmosphere must be avoided during sampling. In the case of CFCs, some sampling materials can introduce contamination (Cook et al. 1995). The widespread industrial use of CFCs also presents problems for their use in industrial and urban environments, where groundwater contamination is likely to occur (Busenberg and Plummer 1992; Böhlke et al. 1997). In the case of  $\text{SF}_6$ , in situ production can occur in some geological formations (Busenberg and Plummer 2000; von Rohden et al. 2010). Elevated concentrations of both CFCs and  $\text{SF}_6$  can occur due to incorporation of excess air during recharge (Heaton and Vogel 1981). Degradation of CFCs (most notably CFC-11 and CFC-113; Cook et al. 1995; Sebol et al. 2007) can also be a problem, leading to over-estimation of groundwater ages. Because these processes affect the different CFCs and  $\text{SF}_6$  to differing extents, their importance can often be determined from a comparison of tracer concentrations.

## $^3\text{H}$

Tritium ( $^3\text{H}$ ) is a radioactive isotope of hydrogen, with a half-life of 12.32 years. Nuclear weapons testing resulted in elevated concentrations of  $^3\text{H}$  in rainfall (in the form of  $^3\text{H}^1\text{HO}$ ) during the 1960s when mean annual  $^3\text{H}$  concentrations reached several hundred times natural levels in the northern hemisphere, and between 5 and 30 times natural levels in the southern hemisphere (Solomon and Cook 1999). Unlike CFCs and  $\text{SF}_6$ , measurement of  $^3\text{H}$  concentration on a single sample does not allow a groundwater age to be assigned, but does indicate groundwater that originated as rainfall since the 1960s. If sufficient samples are collected for the location of high  $^3\text{H}$  concentrations attributable to the 1960s rainfall peak to be identified, then more precise ages can be assigned, and this information can be used to estimate vertical flow velocities and groundwater recharge rates (e.g., Robertson and Cherry 1989). As it moves principally in the liquid phase, residence times determined for  $^3\text{H}$  represent combined unsaturated zone and saturated zone water-residence times. This is in contrast with CFCs and  $\text{SF}_6$ , which predominantly travel through the unsaturated zone in the gas phase (Cook and Solomon 1995). Gas-phase transport in the unsaturated zone is more rapid than liquid-phase transport, and so residence times determined from  $^3\text{H}$  would be expected to be longer than those determined from CFCs and  $\text{SF}_6$ , particularly where the unsaturated zone is thick (Johnston et al. 1998). Travel times of  $^{14}\text{C}$  through the unsaturated zone should be intermediate between those of CFCs,  $\text{SF}_6$  and tritium, because  $^{14}\text{C}$



will move both in the gas phase (as  $\text{CO}_2$ ) and in the liquid phase (as dissolved carbonate).

## Site description

The study area occurs within the Weeli Wolli Creek catchment, near the southern margin of the Hamersley Basin in Western Australia (Fig. 2). The upper catchment is characterised by relatively wide, flat plains, surrounded by hills of outcropping Banded Iron Formation (BIF). The BIF contains one of the largest iron ore deposits in the world, and consequently the area is occupied by a number of large open pit mines. Within the study area, the lower section of the Hamersley Group (primarily the Wittenoom Formation) conformably overlies the Marra Mamba Iron Formation. The iron enrichment in the project area has occurred in the upper section of Marra Mamba Iron Formation, with the ore body ranging from approximately 20–270 m deep, over a strike length of 7 km.

Surface elevation ranges from 580 to 680 m AHD (Australian Height Datum), and Weeli Wolli Creek and its

tributaries drain in a northeast direction, converging at a narrow valley system approximately 30 km down gradient from the headwaters (Fig. 2). The lower catchment downstream of this valley drains on to a wide alluvial floodplain (20–60 km wide), with a meandering channel that can alter its course following large flood events. The region has a highly variable, arid to semi-arid climate, with average daily maximum summer temperatures at Newman between 37 and 39 °C, and average daily maximum winter temperatures between 22 and 25 °C (1965–2003; BOM 2016). Mean annual rainfall at Newman is 318 mm, most of which falls between January and March. Heavy summer storms and tropical cyclones often generate large floods in Weeli Wolli Creek, while winter rainfall is typically not sufficient to generate surface flows.

The main regional aquifer in the study area occurs within the Wittenoom Formation, which consists of interbedded shale, dolomite, sandstone and mudstone. Tertiary detrital and chemical deposits overlie the Wittenoom Formation sediments, and occur within deep valleys (up to 70 m deep) formed by erosion of the Wittenoom Formation. These deposits and the underlying Wittenoom Formation are in

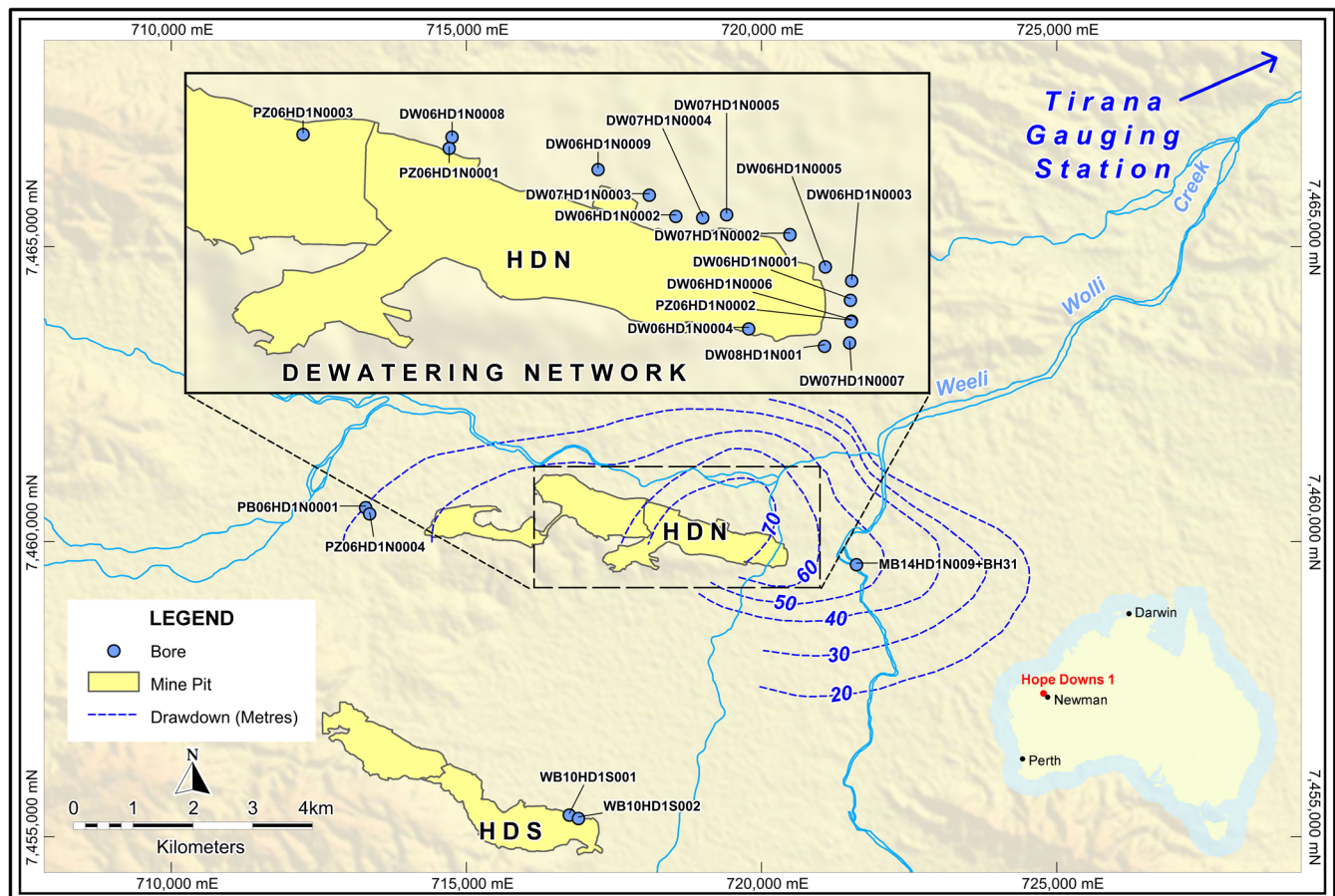


**Fig. 2** Site location map, showing location of Hope Downs North (HDN) and Hope Downs South (HDS) mine pits, Weeli Wolli Creek and floodplain, groundwater monitoring and dewatering bores (blue circles),

and approximate drawdown cone surrounding the Hope Downs North pit in 2015

hydraulic connection with the ore body, creating a significant, high-yielding aquifer system. The base of the aquifer system is the shale units underlying the Wittenoom Formation, at depths of more than 200 m.

The regional hydrogeology is not well understood, as monitoring wells are mostly restricted to the areas immediately surrounding the mine pits; however, pre-mining groundwater elevations suggests groundwater flow from south to north, and discharge to Fortescue Marsh (40 km north of the study site). Infiltration from ephemeral creeks and mountain front recharge are believed to be the principal recharge mechanisms. Over most of the catchment, the water-table depth exceeds 30 m. The groundwater is fresh, with total dissolved solids (TDS) generally 600–700 mg/L, and dominated by magnesium, calcium and bicarbonate ions.

Most mines extend below the natural water table, and the need for dewatering drives the need to understand the source, flow and interconnections between the regional water table, the ore body and nearby groundwater ecosystems. Open pit mining at the study area commenced at Hope Downs North in 2007, with a groundwater abstraction licence of 100 ML/day (megalitres per day) to maintain the groundwater level below the base of the pit. An extensive cone of depression has developed in the vicinity of the mine, with drawdown of over 10 m over an area of  $\sim 8 \text{ km}^2$ , and drawdown of more than 70 m close to the mine (Fig. 3). Mining at Hope Downs South, 5 km further south, commenced in 2010.

Weeli Wolli Creek is ephemeral under natural conditions, although after high rainfall events it can flow for long periods of time. Between 1985 and 2006, the creek flowed 25 % of the time, with a maximum flow duration of 387 days. Since 2007, excess mine water has been discharged into Weeli Wolli Creek about 7.5 km east-northeast of the mine site. Continuous flow now occurs for a distance of 24–27 km downstream of the discharge point (Dogramaci et al. 2015), and baseflow at

Tirana gauging station has steadily increased from approximately  $0.3 \text{ m}^3/\text{s}$  in 2007 to  $1.5 \text{ m}^3/\text{s}$  in 2015.

The chloride concentration of mine water discharged to Weeli Wolli Creek is approximately 75 mg/L; however, this increases downstream due to evaporation. The chloride concentration of flood discharge has not been measured on Weeli Wolli Creek, but was measured on nearby Marillana Creek (20 km further north) during an event in January 2012. At the sampling location, chloride concentration in the creek was initially 150 mg/L (as flow was dominated by mine-water discharge from another mine). Concentrations of 105 and 75 mg/L were measured during the event, although sampling did not correspond with peak flows when chloride concentrations may have been lower. Chloride concentrations in rainfall in the Pilbara were measured on 78 rainfall samples but only eight of these samples were from rainfall events greater than 20 mm. The concentration of conservative chloride ions ranged from 0.5 to 24.9 mg/L, with 98 % of the samples between 0.5 and 5.4 mg/L with a median of 1.3 mg/L (Dogramaci et al. 2012).

## Methods

Samples were collected from 17 production bores—13 bores were sampled in 2008 and 14 bores were sampled in 2014, while 10 bores were sampled in both years. Most of the bores are close to the Hope Downs North mine, although two are close to the Hope Downs South mine. A number of the bores are located on an east–west transect along the northern edge of the Hope Downs North mine pit (Fig. 2). The majority of bores were completed with 300-mm ND steel casing and screens, with construction depths ranging from 120 to 216 m (Table 1). As all of the sampled bores are production bores for mine dewatering, they were constructed with long-screened intervals to maximise yields. Screen lengths range from 72 to 158 m, and in many cases, the water table now occurs within the screened interval. Bores were sampled through a nylon tube that was attached to the production bore taps using brass fittings. Well purging was not required, because wells were pumping at the time of sampling. Groundwater samples for dissolved gases were collected through the tube during submergence of the sample bottles in a bucket, to prevent atmospheric contamination.

In 2008, samples were collected for electrical conductivity, major ion,  $^{18}\text{O}$ ,  $^2\text{H}$ ,  $^{14}\text{C}$ ,  $^{13}\text{C}$  and CFC analysis. In 2014, samples were collected for electrical conductivity, major ion,  $^{18}\text{O}$ ,  $^2\text{H}$ ,  $^{14}\text{C}$ ,  $^{13}\text{C}$ ,  $^3\text{H}$ , CFC and  $\text{SF}_6$  analysis. Samples for  $^{13}\text{C}$  and  $^{14}\text{C}$  analysis were collected in 500-ml HDPE bottles. For samples collected in 2008,  $^{14}\text{C}$  was analysed by Accelerator Mass Spectrometry (AMS) at Australian National University, and  $^{13}\text{C}$  was analysed by either Isotope Ratio Mass Spectrometry (IRMS) at CSIRO Land and Water (7 of 13 samples) or by

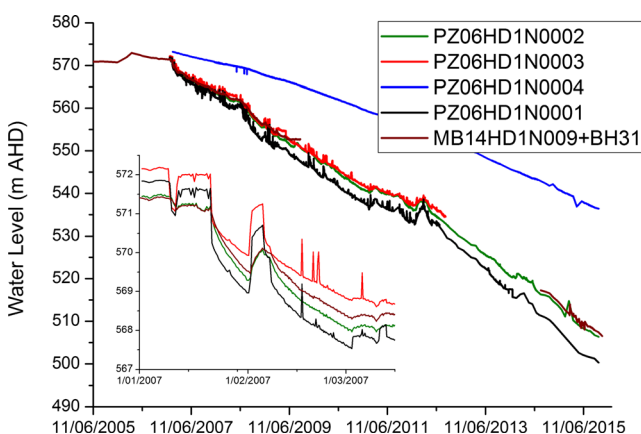


**Fig. 3** Groundwater levels in the vicinity of the Hope Downs North mine. (Bore BH31 was decommissioned in 2009, and replaced by MB14HD1N0009 in 2014.) Bore locations are depicted in Fig. 2

**Table 1** Location of bores and screen intervals

Well	Elevation (m AHD)	Easting	Northing	Screen (m AHD)
DW07HD1N0002	585.8	720254	7460130	393–476
DW07HD1N0005	588.0	719918	7460235	374–511
DW07HD1N0004	587.4	719792	7460219	406–524
DW06HD1N0002	590.3	719650	7460227	422–578
DW07HD1N0003	589.7	719510	7460339	376–470
DW06HD1N0009	591.3	719239	7460475	471–579
DW06HD1N0008	597.4	718466	7460647	436–593
DW06HD1N0001	586.9	720574	7459784	442–575
DW06HD1N0003	592.5	720580	7459887	429–577
DW06HD1N0005	588.6	720441	7459960	422–572
DW07HD1N0007	593.6	720569	7459558	406–524
PB06HD1N0001	625.7	713290	7460601	426–558
WB10HD1S001	615.3	716744	7455391	472–553
WB10HD1S002	612.8	716896	7455332	450–541
DW08HD1N001	594.2	720437	7459540	490–562
DW06HD1N0004	588.2	720035	7459632	464–572
DW06HD1N0006	588.1	720579	7459673	418–574

AMS (6 samples). For samples collected in 2014,  $^{14}\text{C}$  was analysed by AMS and  $^{13}\text{C}$  was analysed by IRMS, both at the GNS Rafter Radiocarbon Laboratory (New Zealand). Carbon-13 isotope data ( $\delta^{13}\text{C}$ ) are reported in delta notation, as per mil (‰) and carbon-14 data are reported as percent modern carbon (pmC) according to the convention described in Stuiver and Polach (1977). Analytical precision (one standard deviation) for  $^{14}\text{C}$  is between 0.1 and 0.3 pmC, and for  $\delta^{13}\text{C}$  is between 0.1 and 0.2 ‰ for samples analysed by IRMS, and between 1.3 and 2.2 ‰ for samples analysed by AMS. Samples for  $^3\text{H}$  analysis were collected in 1-L plastic bottles and measured by electrolytic enrichment and liquid scintillation counting using Quantulus low-level counters (Morgenstern and Taylor 2009). Results are expressed in tritium units (TU), where one TU represents one molecule of  $^3\text{H}^1\text{HO}$  in  $10^{-18}$  atoms of  $\text{H}_2\text{O}$ . The detection limit is 0.025 TU, and standard errors on measurements range from 0.014 to 0.017 TU.

Samples for CFC analysis were collected in 125-ml clear glass bottles with metal screw lids, and analysed for CFC-11, CFC-12 and CFC-113 concentrations by gas chromatography using a purge and trap system with electron capture detector at GNS Water Dating Laboratory, New Zealand. The analytical detection limit of this laboratory for CFCs is approximately 5 pg/kg, although Cook et al. (1995) reported that sampling through nylon tubing could introduce contamination of up to 5 pg/kg for CFC-12 and CFC-113, and up to 20 pg/kg for CFC-11. Cook and Solomon (1997) reported an analytical precision of approximately  $\pm 3$  % for concentrations above 50 pg kg $^{-1}$ ; however, sampling issues for dissolved gases

can be significant, and so precision is sometimes better determined by comparison of results on replicate samples. In the present study, duplicate samples for chlorofluorocarbon analysis were collected on most wells. Approximately 75 % of results on duplicate samples were within 50 % for CFC-11 and CFC-12 (difference between replicates as a percentage of the mean value), and half were within 50 % for CFC-113 (which was only analysed in 2014). This suggests that precision is close to  $\pm 50$  % for the concentrations measured in the present study. Samples for  $\text{SF}_6$  analysis were collected in 1-L glass bottles, and also analysed by gas chromatography at GNS Water Dating Laboratory. The analytical detection limit for  $\text{SF}_6$  is approximately 4 fg/kg, and analytical uncertainties range from 1 to 4 fg/kg for samples analysed in the current study.

Modelling of chlorofluorocarbons and  $\text{SF}_6$  concentrations in water is based on measured atmospheric concentrations at Cape Grimm (Cunnold et al. 1994), converted to equivalent concentrations in water based on the solubilities of these gases (Warner and Weiss 1985; Bu and Warner 1995; Bullister et al. 2002), a recharge elevation of 600 m, and assuming negligible amounts of excess air. A recharge temperature of 24 °C has been assumed, which is the mean annual air temperature for Newman, located 80 km southeast of the mine site.  $^{14}\text{C}$  activities in atmospheric  $\text{CO}_2$  are based on Levin et al. (1992). Long-term records of  $^3\text{H}$  in rainfall are available for Perth (1,000 km to the south) and Darwin (1,700 km to the northeast; Fig. 2).  $^3\text{H}$  activities in rainfall at the study site are assumed to be the mean of Perth and Darwin measurements (Fig. 1; Tadros et al. 2014).

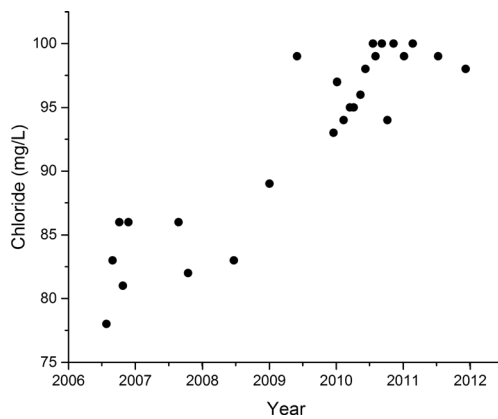


**Fig. 4** Chloride trends in bore DW06HD1N0006 over time

## Results

### Ion concentrations

Chloride concentrations in production bores have been measured since 2007. Figure 4 shows chloride concentrations measured over time in one of these bores. Chloride concentrations increase from 78 mg/L in July 2007 to 100 mg/L in June 2011. Between 2011 and 2012, chloride concentration appears relatively constant. Similar trends are apparent in a number of the other bores.

Total dissolved salt concentrations in groundwater samples collected in 2008 and 2014 range between 460 and 700 mg/L, with bicarbonate as the dominant ion. Chloride concentrations range between 54 and 110 mg/L, with a mean value of 74 mg/L (Table 2). Assuming that groundwater is mainly replenished from diffuse recharge, then based on a mean rainfall of

320 mm and chloride concentration in rainfall of 1.3 mg/L, a recharge rate of approximately 5.6 mm/y is estimated.

### Tracer–tracer plots

#### Carbon-14 and carbon-13

$\delta^{13}\text{C}$  values on groundwater samples collected in 2014 are consistently between 0.9 and 1.7 ‰ more enriched than on those collected in 2008 (mean difference 1.3 ‰; Table 2). The difference is much greater than analytical precision (of IRMS), but might indicate a difference in analytical or sampling protocols between the two sampling times. A relationship of decreasing  $^{13}\text{C}$  value with increasing  $^{14}\text{C}$  activity is apparent in both the 2008 and 2014 data sets (Fig. 5), suggesting addition of carbon from another source; therefore, the variations in  $^{14}\text{C}$  activities cannot be solely ascribed to differences in radioactive decay.

If the relationship between  $^{14}\text{C}$  activity and  $\delta^{13}\text{C}$  value for the 2014 data is extrapolated, the linear trend intersects the 100 pmC line at a  $\delta^{13}\text{C}$  value of approximately  $-17$  ‰. A similar trend line can be drawn through the 2008 data, although the relationship between  $^{14}\text{C}$  and  $\delta^{13}\text{C}$  is less clear for this data set, and so the extrapolation to 100 pmC is less clear. Nevertheless, an initial  $\delta^{13}\text{C}$  activity of  $-17$  ‰ is consistent with a  $\delta^{13}\text{C}$  value of unsaturated zone  $\text{CO}_2$  of  $-25$  ‰, with  $+8$  ‰ fractionation between gaseous  $\text{CO}_2$  and dissolved bicarbonate. The value of  $-25$  ‰ is close to the mean value of  $-23$  ‰ for soil  $\text{CO}_2$  in landscapes dominated by C3 vegetation (Clark and Fritz 1997). The carbonate mineral source could be either dolomite from the aquifer matrix, or soil carbonate.

**Table 2** Results of chemical analyses

Well	2008					2014							
	Cl (mg/L)	$^{14}\text{C}$ (pmC)	$^{13}\text{C}$ (‰)	CFC-11 (pg/kg)	CFC-12 (pg/kg)	Cl (mg/L)	$^{14}\text{C}$ (pmC)	$^{13}\text{C}$ (‰)	CFC-11 (pg/kg)	CFC-12 (pg/kg)	CFC-113 (pg/kg)	$\text{SF}_6$ (fg/kg)	$^3\text{H}$ (TU)
DW07HD1N0002	63	33.0	$-12.6$	23	27	76	41.0	$-11.6$	1.4	7	0	1.5	0.05
DW07HD1N0005	62	31.7	$-12.3$	19	22	73	34.9	$-11.1$	11	29	1.9	9	0.05
DW07HD1N0004	60	31.0	$-12.3$	16	14	67	34.0	$-10.9$	4.1	14	0	4.4	0.09
DW06HD1N0002	62	31.3	$-12.1$	71	12	68	32.3	$-10.7$	18	28	1.9	0	0.02
DW07HD1N0003	59	30.9	$-11.7$	21	22	77	31.8	$-10.8$	4.1	8	0	9	0.00
DW06HD1N0009	59	30.5	$-11.7$	28	19	60	30.8	$-10.7$	2.0	12	0	1.5	0.00
DW06HD1N0008	61	32.2	$-11.6$	20	21	60	31.9	$-10.2$	16	31	4.7	4.4	0.00
DW06HD1N0001	73	43.5	$-13.0$	86	70	81	44.9	$-11.3$	24	29	3.7	0	0.09
DW06HD1N0003	72	40.3	$-13.0$	59	51	61	44.4	$-11.7$	25	35	3.7	4.4	0.10
DW06HD1N0005	69	36.9	$-12.7$	107	40	79	41.4	$-11.4$	12	22	0	2.9	0.03
DW07HD1N0007	—	—	—	—	—	100	37.8	$-11.2$	18	32	5.6	15	0.04
PB06HD1N0001	—	—	—	—	—	54	36.8	$-11.0$	34	33	2.8	2.9	0.01
WB10HD1S001	—	—	—	—	—	110	39.8	$-11.4$	284	34	5.6	76	0.01
WB10HD1S002	—	—	—	—	—	100	35.2	$-10.9$	48	39	4.7	57	0.00
DW08HD1N001	105	37.5	$-13.9$	79	61	—	—	—	—	—	—	—	—
DW06HD1N0004	102	39.0	$-13.9$	285	47	—	—	—	—	—	—	—	—
DW06HD1N0006	83	45.1	$-12.9$	67	52	—	—	—	—	—	—	—	—



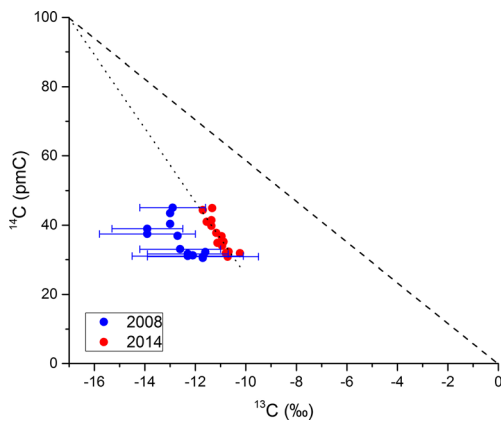


**Fig. 5** Relationship between  $\delta^{13}\text{C}$  and  $^{14}\text{C}$  of dissolved inorganic carbon in groundwater for both 2008 and 2014 sampling periods. The broken line extrapolates the  $^{14}\text{C}$ – $\delta^{13}\text{C}$  trend of the 2014 data to a  $^{14}\text{C}$  value of 100 pmC. Error bars are shown for  $\delta^{13}\text{C}$  values analysed by AMS. For  $^{14}\text{C}$  and  $\delta^{13}\text{C}$  values analysed by IRMS, analytical precision is less than the symbol size

$\delta^{13}\text{C}$  values for Wittenoom Formation dolomite range from  $\sim 2$  to  $2\text{‰}$  (Becker and Clayton 1972).  $\delta^{13}\text{C}$  values of soil carbonates have not been measured within the study area, but are commonly between  $-6$  and  $-8\text{‰}$  (Cerling and Quade 1993). The effect on  $^{14}\text{C}$  values of these two different sources would be different. If observed  $^{14}\text{C}$  activities are not corrected for exchange with carbonate minerals, then apparent  $^{14}\text{C}$  ages would range between 6,500 and 9,900 years. If the source of carbon responsible for enriched  $\delta^{13}\text{C}$  values is the Wittenoom Dolomite ( $\delta^{13}\text{C} \approx 0\text{‰}$ ,  $^{14}\text{C} = 0$ ), then corrected activities (Eq. 4) range between 42 and 68 pmC and corrected ages are between 3,250 and 7,000 years. Alternatively, if the enriched  $\delta^{13}\text{C}$  values of TDIC are predominantly from exchange with soil carbonates ( $\delta^{13}\text{C} \approx -7\text{‰}$ ,  $^{14}\text{C} = 0$ ), then the corrected activities range between 54 and 104 pmC and corrected ages are all less than 5,100 years. If the soil carbonates have  $^{14}\text{C}$  values greater than zero, then the correction would be less than this, and so apparent ages would be greater. In the following, both uncorrected  $^{14}\text{C}$  data and data corrected for exchange with  $^{14}\text{C}$ -dead soil carbonates are therefore presented. In either case, although the mineral source responsible for enrichment of  $\delta^{13}\text{C}$  is ultimately uncertain (as is its  $^{14}\text{C}$  value), these two options bracket the possible range of likely corrections (and hence apparent ages).

### Chlorofluorocarbons, $\text{SF}_6$ and $^3\text{H}$

Figure 6 compares measured concentrations of the tracers that represent groundwater recharged within the past 60 years. Measured values are also compared with expected concentrations based on  $^3\text{H}$  concentrations in rainfall, and groundwater concentrations of dissolved gases in equilibrium with the atmosphere over the past 60 years (Fig. 1). If a sample of rainfall was collected at any time in the past, and concentrations of

two tracers measured, then these concentrations must fall along the equilibrium lines unless they are affected by other geochemical processes (e.g., sorption, degradation, excess air). If a line is drawn connecting any two points on the atmospheric equilibrium line, then sample concentrations along this line are possible by mixing water having these two different ages. The shaded mixing envelope is obtained by drawing all possible mixing lines. Concentrations within the mixing envelopes are possible due to mixing of water having different ages, whereas concentrations falling outside of these envelopes cannot be ascribed solely to mixing processes.

Although CFC-11 and CFC-12 concentrations are low, all CFC-12 values and all but four CFC-11 values are significantly above detection limits. Only two of the 14 wells sampled for CFC-113 concentrations are above the quoted laboratory detection limit of 5 pg/kg, and these only exceed this value by 10 %. There is a significant correlation between CFC-12 and CFC-11, with most samples falling slightly below the equilibrium solubility line, and outside of the mixing envelope. Although these concentrations could be explained by an excess air volume of approximately 40  $\text{cm}^3/\text{kg}$ , this would be inconsistent with  $\text{SF}_6$  data, and also with recent measurements of noble gases which indicate excess air of less than 3  $\text{cm}^3/\text{kg}$ . The data therefore probably indicate some degradation of CFC-11. Degradation of CFC-11 is widely reported in anaerobic environments (Cook et al. 1995; Hinsby et al. 2007), and so CFC-12 and CFC-113 are usually preferred for groundwater dating. Two samples have concentrations significantly above the CFC-11 – CFC-12 equilibrium line and above the mixing envelope, probably indicating contamination of CFC-11.

There is a significant correlation between measured CFC-12 and CFC-113 concentrations, with measurable CFC-113 concentrations only observed where CFC-12 concentrations exceed 25 pg/kg. The samples plot close to the equilibrium solubility line, particularly when the uncertainty of samples at such low concentrations is considered. Samples above the equilibrium line are within the mixing envelope, and could reflect mixing between very young and very old water; however, considering uncertainties of the values at these low concentrations, it is not possible to identify likely mixing end-members.

Only 5 of 14 wells have  $\text{SF}_6$  concentrations above the detection limit, and only two of the  $\text{SF}_6$  measurements are significant (more than three times the analytical uncertainty). Both of these samples plot above the equilibrium solubility line, indicating that  $\text{SF}_6$  is most likely contaminated, with observed concentrations attributed to in situ production (von Rohden et al. 2010).

There is no obvious relationship between CFC-12 and  $^3\text{H}$ , and  $^3\text{H}$  concentrations are below the mixing envelope, which likely reflects the time delay associated with  $^3\text{H}$  movement through the unsaturated zone. Dissolved gases principally move through the unsaturated zone by diffusion within the



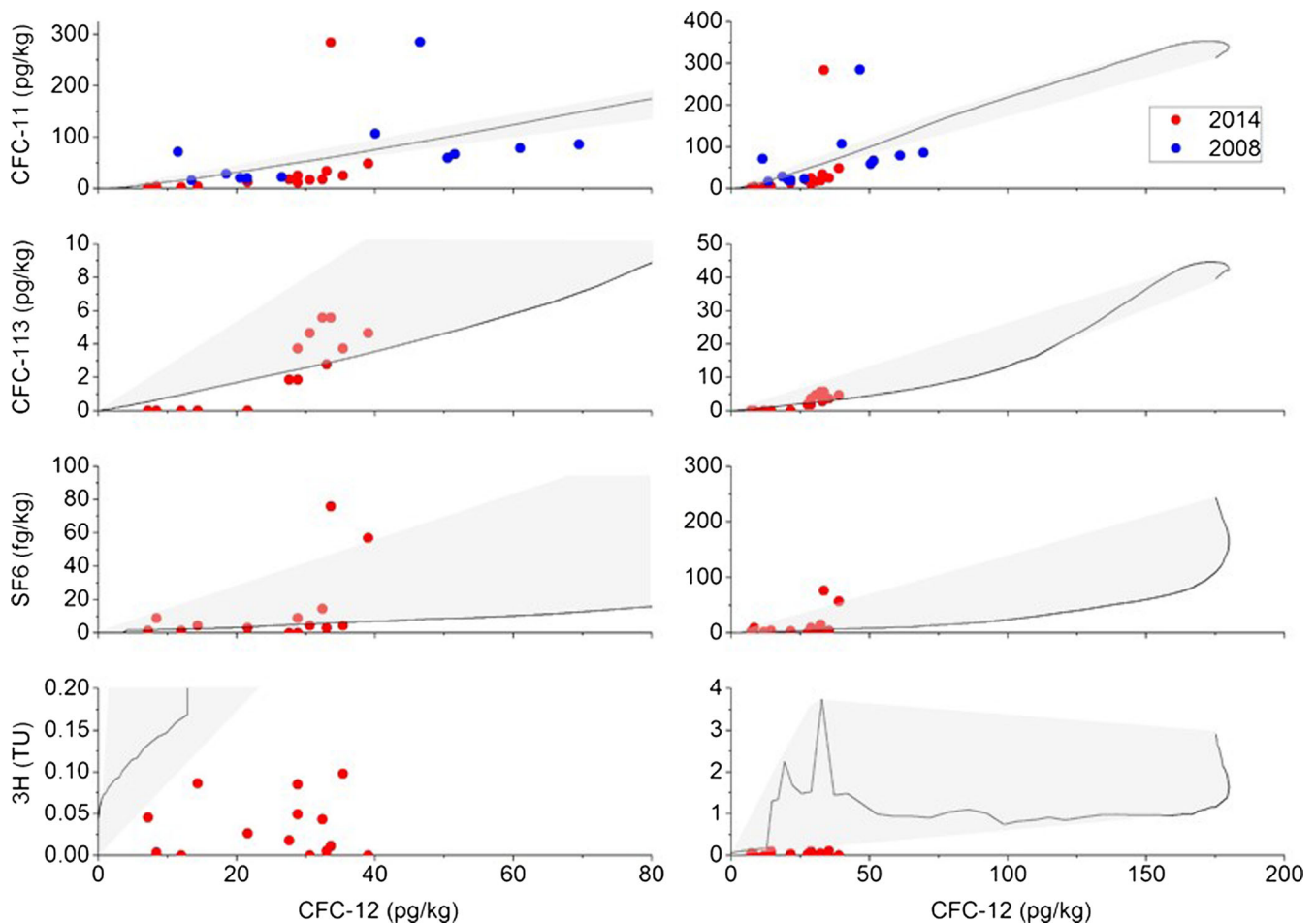


**Fig. 6** Relationship between concentrations of different tracers indicating young (<60 year) residence times. *Solid lines* depict the relationship between concentrations of the tracers for rainfall samples in equilibrium with atmospheric gas concentrations between 1950 and 2014.

gas phase (Cook and Solomon 1995), whereas  $^3\text{H}$  moves principally in the liquid phase. This causes  $^3\text{H}$  to be delayed relative to the dissolved gases, so that  $^3\text{H}$  concentrations are lower than would be expected based on CFC-12 ages (Johnston et al. 1998).

#### $^{14}\text{C}$ , CFC-12 and $^3\text{H}$

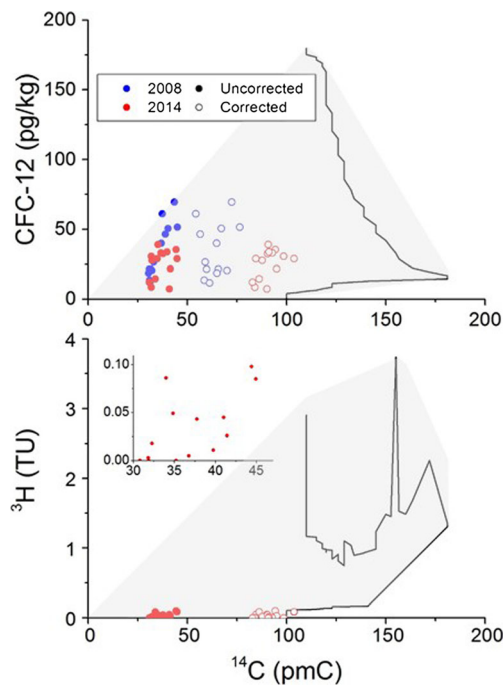
There is a very significant relationship between CFC-12 and uncorrected  $^{14}\text{C}$  for the 2008 samples ( $R^2 = 0.82$ ), but not for the 2014 samples ( $R^2 = 0.07$ ; Fig. 7). The correlation for 2008 samples is also noticeably weaker if the  $^{14}\text{C}$  data is corrected for mineral exchange with  $^{14}\text{C}$ -dead soil carbonate ( $R^2 = 0.06$ ). The correlations between  $^{14}\text{C}$  and  $^3\text{H}$  (2014 only) is significant only if  $^{14}\text{C}$  activities are not corrected ( $R^2 = 0.38$  for uncorrected data, falling to  $R^2 = 0.06$  for corrected data), which may in part reflect the large analytical uncertainty associated with some of the 2008  $\delta^{13}\text{C}$  values, but probably also reflects uncertainty over the correct  $^{14}\text{C}$  correction scheme. Nevertheless, measured concentrations fall within the mixing

These curves assume a temperature of 24 °C, which is the mean air temperature at Newman, a recharge elevation of 600 m and negligible contribution from excess air.) The *shaded regions* indicate concentrations that could arise due to mixing of water of different ages

envelopes, indicating that samples represent mixtures of a small component of young water mixed with old water. Assuming a recharge temperature of 24 °C, the maximum CFC-12 concentration in recharge would have been 180 pg/kg (between 2003 and 2004), and so the measured concentrations of 7–70 pg/kg indicate minimum fractions of young water between 3.9 and 39 %. If the young water fraction was derived outside of 2003–2004 (and hence this end-member had a lower CFC-12 concentration), then the calculated fractions of young water would be greater. The age of the old fraction depends on the correction scheme adopted for  $^{14}\text{C}$ . Mean  $^{14}\text{C}$  activities for the old fraction range between 20 pmC using the uncorrected  $^{14}\text{C}$  data and 85 pmC based on the corrected 2014  $^{14}\text{C}$  data. Corresponding mean ages would be 13,000 and 1,300 years, respectively.

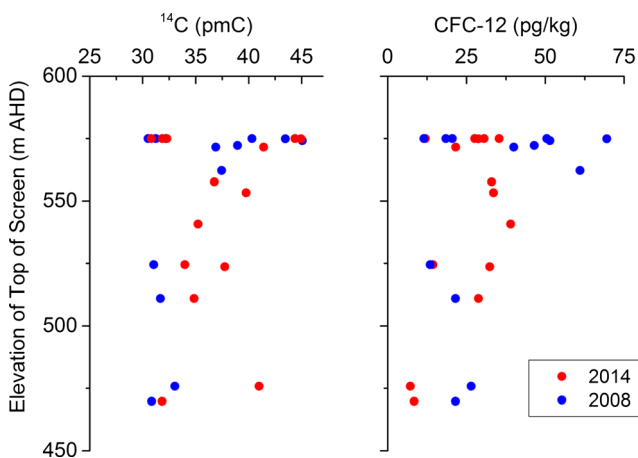
#### Spatial and temporal patterns in tracer concentrations

Figure 8 shows CFC-12 concentrations and uncorrected  $^{14}\text{C}$  activities versus elevation of the top of the well screen. In most



**Fig. 7** Comparison between  $^3\text{H}$  activity, CFC-12 concentration and  $^{14}\text{C}$  activity for 2008 and 2014 samples. Solid lines depict the relationship between concentrations of the tracers for rainfall samples in equilibrium with atmospheric gas concentrations between 1950 and 2014. These curves assume a temperature of 24 °C, which is the mean air temperature at Newman. The shaded regions indicate concentrations that could arise due to mixing of water of different ages. The inset graph shows the relationship between observed  $^{14}\text{C}$  activity and  $^3\text{H}$  concentration in greater detail

cases, higher  $^{14}\text{C}$  activities and CFC-12 concentrations are observed where well screens are shallower. In particular, CFC-12 concentrations above 30 pg/kg are only observed on wells where the top of the screen is located above 560 m, close to the pre-mining water table. Figure 9 plots the same data (but also



**Fig. 8** Observed  $^{14}\text{C}$  activities and CFC-12 concentrations versus elevation of the top of the well screen. (Where the elevation of the screen top was above the water table prior to commencement of dewatering, data are plotted versus the nominal pre-mining water table depth of 575 m AHD)

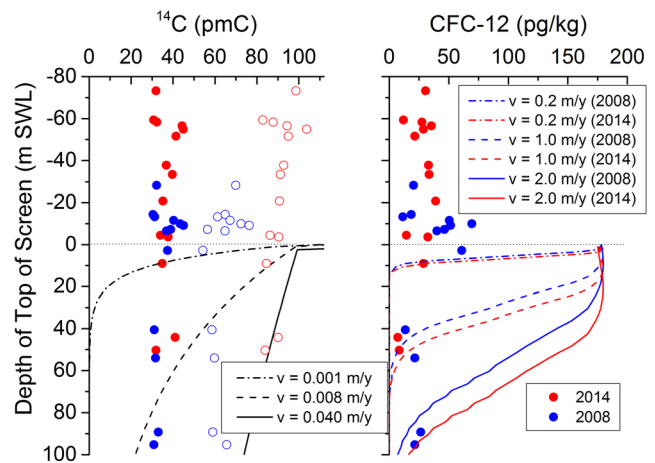


**Fig. 9**  $^{14}\text{C}$  activity and CFC-12 concentrations plotted against top of screen, relative to the water-table position at time of sampling (assumed to be 565 m AHD in 2008 and 520 m AHD in 2014). Negative values indicate situations where top of the screen occurs above the water table. (The dotted horizontal line indicates the water table position.) Curved lines indicate expected concentrations based on advective transport with a vertical velocity of between 0.001 and 0.04 m/y ( $^{14}\text{C}$ ) and between 0.2 and 2 m/y (CFC-12). Assuming an effective porosity of 0.2, vertical water velocities of 0.001–0.04 m/y are equivalent to recharge rates of between 0.0002 and 0.008 m/y, and velocities of 0.2–2.0 m/y are equivalent to recharge rates between 0.04 and 0.4 m/y. (For CFC-12, blue lines show expected concentrations in 2008, whereas red lines show expected concentrations in 2014. For  $^{14}\text{C}$ , model curves for 2008 and 2014 are indistinguishable)

including corrected  $^{14}\text{C}$  activities) versus the depth of the top of the screen below the water table at the time of sampling, and also compares this with expected values based on uniform vertical velocities. These theoretical curves have been derived from atmospheric input concentrations (Fig. 1), and assuming vertical piston flow. They therefore do not include the effects of dispersion, although this would be relatively small at these velocities (Walker and Cook 1991; Ekwurzel et al. 1994). Vertical water velocities of between 0.008 and 0.04 m/y are required to explain much of the corrected  $^{14}\text{C}$  data, whereas some of the CFC-12 data require vertical velocities of more than 2 m/y. Assuming an effective porosity of 0.2, vertical water velocities of 0.008–0.04 m/y are equivalent to recharge rates of between 0.0016 and 0.008 m/y, and a velocity of 2.0 m/y is equivalent to a recharge rate of 0.4 m/y.

One of the difficulties of interpreting tracer data from long-screened wells is that the depth of origin of sampled groundwater is uncertain. Where the top of the well screen occurs above the water table, tracer data cannot be used to estimate water velocities without making assumptions about the depth of origin of the water samples from within the screened intervals. For the rest of the data, comparison with model curves (Fig. 9) indicates minimum vertical velocities. These minimum velocities would be true velocities if water were sourced only from the top of the well screen. Greater velocities would be estimated if water is sourced from deeper parts of the

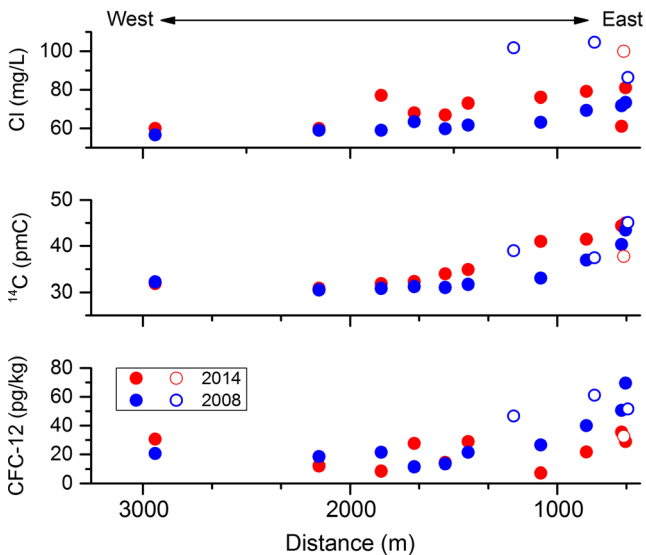


**Fig. 10** Cl concentration,  $^{14}\text{C}$  activity and CFC-12 concentration versus distance from the Weeli Wolli floodplain. *Solid symbols* denote wells that were sampled in both 2008 and 2014, and *open symbols* denote wells that were sampled on only one occasion. Uncorrected  $^{14}\text{C}$  activities are plotted here, so that small differences in  $^{14}\text{C}$  activities are not masked by uncertainties in  $\delta^{13}\text{C}$  values

screened interval. Also, if the water samples are mixtures with young and old components, then even greater velocities would be required for the young fraction. Such high vertical water velocities are unlikely to reflect diffuse recharge processes, and this is discussed further in the following.

One of the limitations of the dataset is that wells with shallow screens are preferentially located to the east of the transect, which makes it difficult to distinguish vertical trends from horizontal trends; thus, concentrations of  $^3\text{H}$ , CFC-12, and  $^{14}\text{C}$  activities all show a decreasing trend with distance from the Weeli Wolli Creek floodplain (Fig. 10). It is also noteworthy that significant changes in concentrations of some of the environmental tracers are observed between 2008 and 2014, and these may be due to hydrological changes induced by mine dewatering. In particular,  $^{14}\text{C}$  activities increased in all wells, and these increases are most significant to the east of the transect (Fig. 10). The pattern is less clear for CFC-12, with some data showing reductions in concentrations between sampling times and others showing increases. The increased  $^{14}\text{C}$  activities in 2014 suggest that the travel time to the wells close to the floodplain has decreased.

## Discussion

### Conceptual model for groundwater flow

The presence of above-background concentrations of CFCs and  $^3\text{H}$  at significant depths (i.e., where the top of the well

screen is more than 40 m below the water table at the time of sampling) is difficult to explain in terms of diffuse recharge to aquifers with high porosity. A number of previous studies have reported very young apparent groundwater ages at considerable depth in systems dominated by flow through fractures (e.g., Cook et al. 2005), but this is not consistent with the conceptual model of the field site. Rather, it is possible that the high vertical water velocities necessary to move young water to these depths occur in areas of localised recharge. Infiltration beneath Weeli Wolli Creek is one such potential localised recharge source.

Infiltration rates from Weeli Wolli Creek and nearby Marilana Creek have been measured during steady flow conditions generated by mine-water discharge as the difference between total loss rate (obtained from flow gauging) and evapotranspiration (Dogramaci et al. 2015; Bourke et al. 2014). Where the streams are losing, infiltration rates of 2.6–6.8  $\text{m}^2/\text{d}$  have been measured, equivalent to vertical velocities of 1.5–3.5  $\text{m}/\text{d}$  based on a stream width of 10 m and porosity of 0.2. Infiltration rates during natural flow events have not been measured, but are likely to be much higher. Prior to mine-water discharge, Weeli Wolli Creek flowed 25 % of the time at the Tirana gauging station, suggesting velocities of 70–200  $\text{m}/\text{y}$ . Of course, vertical water velocities would decrease with depth below the water table due to curvature of flowlines away from the creek, but the aforementioned calculation does indicate the potential for very high velocities.

Changes in groundwater age with time have been measured in the east of the well transect, close to Weeli Wolli Creek. Prior to mining, the regional gradient at the mine site was from west to east, and hydraulic head in PZ06HD1N0001 (located 3 km west of Weeli Wolli Creek floodplain) was approximately 0.5 m above that in BH31 (located at the edge of the creek floodplain; Fig. 2). However, within a few months of the commencement of pumping, groundwater levels at the edge of the floodplain had been lowered by more than 2 m. By 2014, the groundwater level on the edge of the floodplain had been lowered by 50 m. The total volume of groundwater pumped till 2015 is approximately  $3 \times 10^8 \text{ m}^3$ . Assuming that the cone of depression is circular, and also assuming an aquifer thickness of  $h = 100 \text{ m}$  and porosity of  $\varepsilon = 0.2$ , this would induce flow to the well field from a radial distance of approximately 2,000 m (using  $Q = \pi r^2 h \varepsilon$ ; where  $Q$  is the total volume pumped and  $r$  is the radial distance). This is therefore consistent with the increase in  $^{14}\text{C}$  activity being due to an increase in flow of young groundwater from beneath the creek. The increase in chloride concentration observed in dewatering bores may also be due to an increase in water sourced from river infiltration, although further sampling of river floodwaters would be required to confirm this. Assuming a pumping rate of  $4 \times 10^7 \text{ m}^3/\text{y}$ , water would have been drawn in over a distance of approximately 1,200 m in 3 years, which is consistent with the increase in chloride concentration occurring in

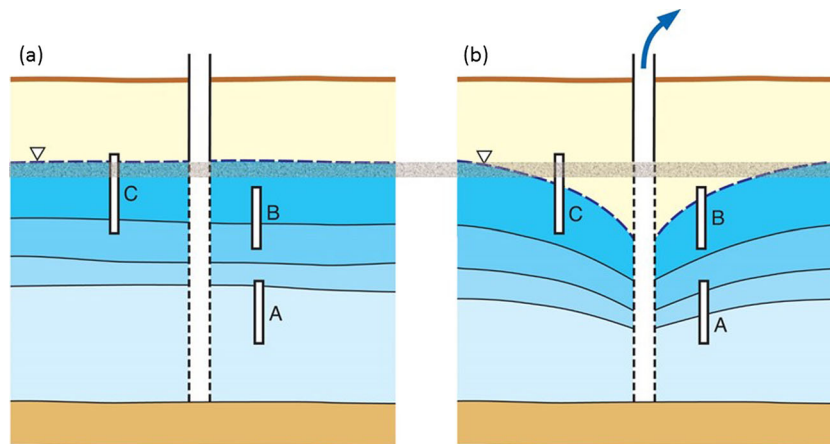


**Fig. 11** Schematic representation of groundwater ages **a** before, and **b** during groundwater pumping. If groundwater age varies with depth, but not laterally, then pumping-induced drawdown from a fully screened well should compress the age contours so that the proportion of aquifer thickness within each age range is unchanged. Groundwater ages in observation wells will change depending on the location of the well screen relative to the extent of drawdown. **A** The groundwater age would expected to decrease during pumping, although ages may be

beyond the limit of dating with CFCs. **B** The groundwater age decreases during pumping. **C** Although the mean groundwater age within the screened interval decreases, before pumping the top of the well screen coincided with a highly permeable layer (indicated by shaded area) and so the youngest water was preferentially sampled. Since this is no longer the case, the apparent age may increase with pumping

2010, 3 years after pumping commenced. Chloride concentrations measured in recent samples are consistent with measured chloride concentrations in flood discharge.

Changes in CFC-12 with time are less consistent than changes in  $^{14}\text{C}$ . For  $^{14}\text{C}$ , all wells show an increase in activity, although it is more pronounced to the east of the transect. For CFC-12 some bores show an increase, whereas others show a decrease. This may be related to the depth of well screens relative to the drawdown (Fig. 11). Of the ten bores that were sampled in both 2008 and 2014, the screens for two of these remain below the water table despite drawdown of more than 70 m. These bores do not show an increase in CFC-12 concentration, and the concentration measured in 2014 is less than 10 pg/kg (and may be close to background; well A in Fig. 11). Where the water table was significantly above the well screen in 2008 but within the screened interval in 2014, CFC-12 concentrations would be expected to increase. Young water would occur close to the water table prior to pumping, and while the zone of young water may be compressed by the reduction in aquifer thickness caused by drawdown, water near the water table should still be young. Two wells fall into this category: one shows a significant increase in CFC-12 concentration, and the other shows a small increase. There are six wells whose screens intercepted the water table at the time of sampling in 2008. Two of these show significant increases in CFC-12 concentration, but four show decreases. An increase in CFC-12 concentration might be caused by a reduction in the volume of old water sampled by these wells (well B in Fig. 11), but a decrease in concentration is more difficult to explain and is possibly due to a decrease in permeability with depth within the screened intervals of the wells. Thus,

although young water would have been within the screened interval of these wells in both 2008 and 2014, the young water would have been preferentially sampled in 2008 (as it was associated with a shallow high permeability zone; well C in Fig. 11).

#### Aquifer recharge rates

A preliminary estimate of the diffuse aquifer recharge rate can be obtained from the estimated  $^{14}\text{C}$  activity of the old end-member of between 20 (uncorrected) and 85 (corrected) pmC. If the uncorrected  $^{14}\text{C}$  activity of this end-member is attributed to radioactive decay from an initial activity of 100 pmC, then the apparent age is estimated to be approximately 13,000 years. The average depth of production well screens below the pre-mining water table is approximately 85 m, giving an apparent mean vertical water velocity of 6.5 mm/y and recharge rate of 1.3 mm/y assuming one-dimensional flow and a porosity of 0.2. In comparison, if it is assumed that the  $^{14}\text{C}$  activity is affected by exchange with  $^{14}\text{C}$ -dead soil carbonate, then the apparent age of this end-member is estimated to be 1,300 years, and the recharge rate would be 13 mm/y. Of course, this is probably an underestimate of the actual diffuse recharge rate for a number of reasons. Firstly, it has been assumed that groundwater is derived from the midpoint of the well screens. Hydraulic conductivity often decreases with depth, and if this is the case then the water would have been predominantly derived from shallower depths. Also, the vertical velocity usually decreases with depth in a two-dimensional flow field, so that the vertical velocity at the water table would have been higher than estimated. Both of



these assumptions would result in an estimate of recharge that is lower than the true value.

The diffuse recharge rate was independently estimated to be 5.6 mm/y based on a chloride mass balance. This estimate is also subject to a number of assumptions. Groundwater is believed to be a mixture of diffuse recharge and creek recharge. As there is some evidence that creek recharge has a higher chloride concentration than diffuse recharge, not accounting for this mixing process may result in a slight underestimate of recharge; however, other assumptions may be more significant. The chloride mass balance approach assumes that all chloride fallout within the catchment exits the catchment through groundwater. In the Weeli Wolli catchment, surface-water outflow occurs through the naturally ephemeral Weeli Wolli Creek. Mean annual flow of Weeli Wolli Creek measured at the Tarina gauging station prior to mining is approximately  $1.4 \times 10^7 \text{ m}^3/\text{y}$  (1985–2006), and the catchment area above the gauging station is 1,512 km<sup>2</sup>. This therefore represents a mean annual runoff of 9 mm/y. It is often assumed that the concentration of chloride in runoff is equal to that in precipitation, and if this is the case then the chloride loss from the catchment will be very small and so will not greatly affect the chloride mass balance calculation. However, it is possible that chloride concentrations in runoff are higher than those in precipitation, which may mean that the chloride mass balance is an overestimation of the recharge rate; thus, this requires further analysis. Nevertheless, considering the inherent assumptions of both the <sup>14</sup>C and chloride mass balance estimates of recharge, the two are considered to be in reasonable agreement.

### Outstanding issues and further work

Interpretation of environmental tracer concentrations measured in dewatering bores in the vicinity of open pit mines is complicated by long-screened intervals of bores, and transient changes in the flow system. Also, most available bores are located within a close proximity of the mine site, and there is poor coverage across the catchment. Constructing a defensible conceptual model with these limitations is difficult. Nevertheless, available data are consistent with a change in flow direction induced by groundwater pumping, so that localised recharge from Weeli Wolli Creek now forms a larger proportion of the pumped groundwater. However, a number of additional studies are needed to confirm these findings, and to more clearly define flow systems and recharge rates. Although these recommendations relate specifically to the field site studied in the current report, they underlie the uncertainties created by sampling long-screened wells to define transient flow systems.

1. Estimation of vertical water velocities and hence aquifer recharge rates from environmental tracer data is compromised by the large-screened intervals of wells. Although the use of multiple tracers has been applied in previous studies to infer mixing in long-screened wells (e.g., Visser et al. 2013), this is limited by the availability of tracers. This approach also requires that individual tracer concentrations can be very accurately resolved, and this is not always possible. Although the present study used six different tracers of groundwater age, resolution was limited because (1) five of these tracers are sensitive to the same time period (<60 years), and (2) resolution was poor with many tracers, as concentrations were close to background, and hence measurement uncertainties were large. Uncertainty in the initial activity of <sup>14</sup>C also proved to be a limitation. Measurements of additional tracers that are sensitive to different time periods, including dissolved helium (Solomon et al. 1996) and <sup>39</sup>Ar (Visser et al. 2013), would assist discrimination of mixing patterns, and is currently planned.
2. An alternative approach might be to infer intake zones of piezometers by determining depth profiles of hydraulic conductivity. Although access to dewatering bores for packer sampling or similar testing is not possible at the project site (as pumps are permanently installed), there are a number of monitoring piezometers adjacent to some of the dewatering bores that have similar screened intervals. Measurements of the vertical distribution of hydraulic conductivity in these piezometers may provide valuable information on the likely intake zones within the screened intervals of the wells. This will help determine the depth of the groundwater samples obtained from these large-screened intervals. The information may also allow us to assess whether the proportion of water obtained from different depths has changed as the water table has declined (Mayo 2010).
3. Changes in the flow system would not have been identified if tracer concentration data from different sampling times were not available. Repeated sampling of environmental tracers as the mining continues and groundwater levels continue to decline will help to assess the changes in groundwater age with time, and should confirm or refute the current conceptual model. Temporal sampling is also a valuable tool for identifying age distributions of mixed groundwater samples (McCallum et al. 2014).
4. Most analytical models for interpreting groundwater age assume steady-state flow conditions (Vogel 1967; Cook and Bohlke 2000), and so numerical models are necessary for transient flow systems. Numerical models of drawdown in the vicinity of the mine pits have been developed for operational purposes. Extending these models to catchment-scale and simulating groundwater age distributions will also assist evaluation and further development of the conceptual model of the site.
5. Determining sources of groundwater requires accurate definition of end-members. Measurement of tracer

concentrations in creek infiltration (particularly Cl and  $\delta^{13}\text{C}$ ) will help determine whether the increase in chloride concentration observed in production bores is consistent with capture of creek infiltration.

## Conclusions

Temporal sampling of multiple environmental tracers has identified mixing of young and old groundwater, and transient changes in the flow system.  $^3\text{H}$  and CFC-12 concentrations and  $^{14}\text{C}$  activity all decrease with depth, but also increase towards Weeli Wolli Creek. It is therefore hypothesised that young water that recharges the aquifer beneath Weeli Wolli Creek has been pulled into the dewatering bores. Simple estimates of travel time suggest this water could have reached the dewatering bores within a few years of pumping having commenced. Although it is not possible to estimate the rate of creek recharge, preliminary estimates of diffuse recharge can be derived from the  $^{14}\text{C}$  activity of the old water component and from a chloride mass balance. Estimates obtained from these different methods are in reasonable agreement given the assumptions inherent in each method and the limitations of the available data. They suggest a diffuse recharge rate between 1 and 13 mm/y. Increases in  $^{14}\text{C}$  activity and chloride concentrations between 2008 and 2014 suggest that the proportion of pumped groundwater derived from creek recharge is increasing.

**Acknowledgements** This work was undertaken as part of a collaborative project between the National Centre for Groundwater Research and Training (NCGRT) and Rio Tinto Iron Ore. Funding was provided by the Australian Research Council, through Linkage Grant LP150100395 and by Rio Tinto Iron Ore. We thank several members of our teams at RTIO and Flinders University whose work made this study possible, especially Glenn Kirkpatrick for assistance in the field, Maree Swebbs and Thomas Linklater for help with the map preparations.

## References

- Allison GB, Gee GW, Tyler SW (1994) Vadose-zone techniques for estimating groundwater recharge in arid and semiarid regions. *Soil Sci Soc Am J* 58(1):6–14
- Becker RH, Clayton RN (1972) Carbon isotopic evidence for the origin of a banded iron formation in Western Australia. *Geochim Cosmochim Acta* 36:577–595
- Böhlke JK, Revesz K, Busenberg E, Deak J, Deseo E, Stute M (1997) Groundwater record of halocarbon transport by the Danube River. *Environ Sci Technol* 31(11):3293–3299
- BOM (2016) Climate statistics for Australian locations. [http://www.bom.gov.au/climate/averages/tables/cw\\_007151.shtml](http://www.bom.gov.au/climate/averages/tables/cw_007151.shtml). Australian Government, Bureau of Meteorology. Accessed 29 July 2016
- Bourke SA, Cook PG, Shanafield M, Dogramaci S, Clark JF (2014) Characterisation of hyporheic exchange in a losing stream using radon-222. *J Hydrol* 519:94–105
- Bu X, Warner MJ (1995) Solubility of chlorofluorocarbon 113 in water and seawater. *Deep-Sea Res* 42(7):1151–1161
- Bullister JL, Wisegarver DP, Menzia FA (2002) The solubility of sulfur hexafluoride in water and seawater. *Deep-Sea Res* 49:175–187
- Busenberg E, Plummer LN (1992) Use of chlorofluorocarbons ( $\text{CCl}_3\text{F}$  and  $\text{CCl}_2\text{F}_2$ ) as hydrologic tracers and age-dating tools: the alluvium and terrace system of central Oklahoma. *Water Resour Res* 28(9):2257–2283
- Busenberg E, Plummer LN (2000) Dating young groundwater with sulfur hexafluoride: natural and anthropogenic sources of sulfur hexafluoride. *Water Resour Res* 36(10):3011–3030
- Cerling TE, Quade J (1993) Stable carbon and oxygen isotopes in soil carbonates. In: *Climate change in continental isotopic records*. Geophysical Monograph 78, American Geophysical Union, Washington, DC, pp 217–231
- Clark ID, Fritz P (1997) *Environmental isotopes in hydrogeology*. Lewis, Boca Raton, FL
- Cook PG, Bohlke JK (2000) Determining timescales for groundwater flow and solute transport. In: Cook PG, Herczeg AL (eds) *Environmental tracers in subsurface hydrology*. Kluwer, Boston, pp 1–30
- Cook PG, Solomon DK (1995) The transport of atmospheric trace gases to the water table: implications for groundwater dating with chlorofluorocarbons and krypton-85. *Water Resour Res* 31:263–270
- Cook PG, Solomon DK (1997) Recent advances in dating young groundwater:  $^3\text{H}/^3\text{He}$ , chlorofluorocarbons and  $^{85}\text{Kr}$ . *J Hydrol* 191:245–265
- Cook PG, Solomon DK, Plummer LN, Busenberg E, Schiff SL (1995) Chlorofluorocarbons as tracers of groundwater transport processes in a shallow, silty sand aquifer. *Water Resour Res* 31(3):425–434
- Cook PG, Love AJ, Robinson NI, Simmons CT (2005) Groundwater ages in fractured rock aquifers. *J Hydrol* 308:284–301
- Cornaton FJ (2012) Transient water age distributions in environmental flow systems: the time-marching Laplace transform solution technique. *Water Resour Res* 48(3). doi:10.1029/2011WR010606
- Cunnold DM, Fraser PJ, Wiess RF, Prinn RG, Simmonds PG, Miller BR, Alyea FN, Crawford AJ (1994) Global trends and annual releases of  $\text{CCl}_3\text{F}$  and  $\text{CCl}_2\text{F}_2$  estimated for ALE/GAGE and other measurements from July 1978 to June 1991. *J Geophys Res Atmos* 99(D1):1107–1126
- Dogramaci S, Skrzypek G, Dodson W, Grierson PF (2012) Stable isotope and hydrochemical evolution of groundwater in the semi-arid Hamersley Basin of subtropical northwest Australia. *J Hydrol* 475:281–293
- Dogramaci S, Firmani G, Hedley P, Skrzypek G, Grierson PF (2015) Evaluating recharge to an ephemeral dryland stream using a hydraulic model and water, chloride and isotope mass balance. *J Hydrol* 521:520–532
- Dunkle SA, Plummer LN, Denver JM, Hamilton PA, Michel RL, Coplen TB (1993) Chlorofluorocarbons ( $\text{CCl}_3\text{F}$  and  $\text{CCl}_2\text{F}_2$ ) as dating tools and hydrologic tracers in shallow groundwater of the Delmarva Peninsula, Atlantic Coastal Plain, United States. *Water Resour Res* 29(12):3837–3860
- Eberts SM, Kauffman LJ, Jurgens BC (2012) Comparison of particle-tracking and lumped-parameter age-distribution models for evaluating vulnerability of production wells to contamination. *Hydrogeol J* 20:263–282
- Ekwurzel B, Schlosser P, Smethie WM, Plummer LN, Busenberg E, Michel RL, Weppernig R, Stute M (1994) Dating of shallow groundwater: comparison of the transient tracers  $^3\text{H}/^3\text{He}$ , chlorofluorocarbons, and  $^{85}\text{Kr}$ . *Water Resour Res* 30(6):1693–1708
- Heaton THE, Vogel JC (1981) “Excess air” in groundwater. *J Hydrol* 50:201–216
- Hinsby K, Hojberg AL, Engesgaard P, Jensen KH, Larsen F, Plummer LN, Busenberg E (2007) Transport and degradation of

- chlorofluorocarbons (CFCs) in the pyritic Rabis Creek aquifer, Denmark. *Water Resour Res* 43(10). doi: [10.1029/2006WR005854](https://doi.org/10.1029/2006WR005854)
- Ingerson R, Pearson FJ (1964) Estimation of age and rate of motion of groundwater by the  $^{14}\text{C}$  method. In: Miyake Y, Koyama T (eds) Recent research in the field of hydrosphere. In: Atmosphere and nuclear geochemistry. Marusen, Tokyo, pp 263–283
- Johnston CT, Cook PG, Frape SK, Plummer LN, Busenberg E, Blackport RJ (1998) Groundwater age and nitrate distribution within a glacial aquifer beneath a thick unsaturated zone. *Groundwater* 36(1):171–180
- Jurgens BC, Bexfield LM, Eberts SM (2014) A Ternary age-mixing model to explain contaminant occurrence in a deep supply well. *Groundwater* 52:25–39
- Leray S, de Dreuzay JR, Aquilina L, Vergnaud-Ayraud V, Labasque T, Bour O, Le Borgne T (2014) Temporal evolution of age data under transient pumping conditions. *J Hydrol* 511:555–566
- Levin I, Bössinger R, Bonani G, Francey RJ, Kromer B, Munnich KO, Suter M, Trivett NBA, Wöflfi W (1992) Radiocarbon in atmospheric carbon dioxide and methane: global distribution and trends. In: Taylor RE, Long A, Kra RS (eds) Radiocarbon after four decades, Springer, Heidelberg, Germany, pp 503–518
- Manning AH, Clark JF, Diaz SH, Rademacher LK, Earman S, Plummer LN (2012) Evolution of groundwater age in a mountain watershed over a period of thirteen years. *J Hydrol* 460–461:13–28
- Massoudieh A (2013) Inference of long-term groundwater flow transience using environmental tracers: a theoretical approach. *Water Resour Res* 49(12):8039–8052
- Mayo AL (2010) Ambient well-bore mixing, aquifer cross-contamination, pumping stress and water quality from long-screened wells: what is sampled and what is not? *Hydrogeol J* 18(4):823–827
- McCallum JL, Engdahl NB, Ginn TR, Cook PG (2014) Non-parametric estimation of groundwater residence time distributions: what can environmental tracer data tell us about groundwater residence time? *Water Resour Res* 50(3):2022–2038
- McMahon PB, Plummer LN, Bohlke JK, Shapiro SD, Hinkle SR (2011) A comparison of recharge rates in aquifers of the United States based on groundwater-age data. *Hydrogeol J* 19(4):779–800
- Morgenstern U, Taylor CB (2009) Ultra low-level tritium measurement using electrolytic enrichment and LSC. *Isotopes Environ Health Stud* 45(2):96–117
- Pearson FJ, White DE (1967) Carbon 14 ages and flow rates of water in Carrizo Sand, Atascosa County, Texas. *Water Resour Res* 3(1):251–261
- Robertson WD, Cherry JA (1989) Tritium as an indicator of recharge and dispersion in a groundwater system in central Ontario. *Water Resour Res* 25(6):1097–1109
- Sebol LA, Robsertson WD, Busenberg E, Plummer LN, Ryan MC, Schiff SL (2007) Evidence of CFC degradation in groundwater under pyrite-oxidizing conditions. *J Hydrol* 347(1–2):1–12
- Solomon DK, Cook PG (1999)  $^3\text{H}$  and  $^3\text{He}$ . In: Cook PG, Herczeg AL (eds) Environmental tracers in subsurface hydrology. Kluwer, Boston, pp 397–424
- Solomon DK, Sudicky EA (1991) Tritium and helium-3 isotopic ratios for direct estimation of spatial variations in groundwater recharge. *Water Resour Res* 27(9):2309–2319
- Solomon DK, Hunt A, Poreda RJ (1996) Source of radiogenic helium 4 in shallow aquifers: implications for dating young groundwater. *Water Resour Res* 32(6):1805–1813
- Stuiver M, Polach HA (1977) Discussion: reporting of carbon-14 data. *Radiocarbon* 19:355–363
- Tadros CV, Hughes CE, Crawford J, Hollins SE, Chisari R (2014) Tritium in Australian precipitation: a 50 year record. *J Hydrol* 513:262–273
- Tamers MA (1967) Radiocarbon ages of groundwater in an arid zone unconfined aquifer. In: Isotope techniques in the hydrological cycle. AGU Monograph 11, AGU, Washington, DC, pp 3–152
- Varni M, Carrera J (1998) Simulation of groundwater age distributions. *Water Resour Res* 34(12):3271–3281
- Visser A, Broers HP, Purtschert R, Sultenfuß J, de Jonge M (2013) Groundwater age distributions at a public drinking water supply well field derived from multiple age tracers ( $^{85}\text{Kr}$ ,  $^3\text{H}/^3\text{He}$ ,  $^{39}\text{Ar}$ ). *Water Resour Res* 49:7778–7796. doi:[10.1002/2013WR014012](https://doi.org/10.1002/2013WR014012)
- Vogel JC (1967) Investigation of groundwater flow with radiocarbon. In: Isotopes in hydrology. IAEA, Vienna, pp 355–369
- von Rohden C, Kreuzer A, Chen Z, Aeschbach-Hertig W (2010) Accumulation of natural  $\text{SF}_6$  in the sedimentary aquifers of the North China Plain as a restriction on groundwater dating. *Isot Environ Health Stud* 46(3):279–290
- Walker GR, Cook PG (1991) The importance of considering diffusion when using carbon-14 to estimate groundwater recharge. *J Hydrol* 128:41–48
- Warner MJ, Weiss RF (1985) Solubilities of chlorofluorocarbons 11 and 12 in water and seawater. *Deep-Sea Res* 32(12):1485–1497
- Weissmann GS, Zhang Y, Labolle EM, Fogg GE (2002) Dispersion of groundwater age in an alluvial aquifer system. *Water Resour Res* 38(10):1198. doi:[10.1029/2001WR000907](https://doi.org/10.1029/2001WR000907)